



Assessment of a house affected by ground movement using terrestrial laser scanning and numerical modeling

Xugang Lian^{1,3} · Huayang Dai² · Linlin Ge³ · Yinfei Cai¹

Received: 7 March 2019 / Accepted: 6 April 2020 / Published online: 19 April 2020
© Springer-Verlag GmbH Germany, part of Springer Nature 2020

Abstract

This study analyzed the internal mechanical state of houses disturbed by underground coal mining, especially those that are free from damage in subsidence areas. Traditional surveying and terrestrial laser scanning (TLS) were utilized as the external monitoring methods to obtain the outside displacement of the disturbed houses. The results were then used to estimate the internal mechanical state of houses using simulation software. Three high-quality houses in Paifang Village, China were scanned using TLS in their pre- and post-mining stages. The magnitude of movement and deformation was highly related to the location of the building in the panel, which was enlarged near the center of the subsidence basin. ANSYS was used to compute the internal state of the houses with a focus on the structural columns, ring beams, and walls of the houses under changing tensile conditions. Results showed that the structural column and ring beam can resist tensile deformation, whereas the window corner was the principal point of stress concentration with potential risk of cracking. Mastering the internal stress state of undamaged buildings in mining-affected areas can help to strengthen the pre-maintenance of houses and guide the construction of new anti-deformation houses. The results of this work may benefit the construction of anti-deformation buildings in mining regions.

Keywords Traditional surveying · Terrestrial laser scanning · Numerical simulation · Internal mechanical state of houses · Underground coal mine

Introduction

Coal is located in a certain position of underground rock mass, contacts with the surrounding rock mass, and maintains its stress equilibrium state. After the underground coal seam is extracted, the strata around the mining space lose their support and gradually move to the panel and destroy. With the continuous expansion of mining space, this moving process gradually expands from the position of the mining space to the periphery and upward, until it spreads to the surface, causing surface subsidence and horizontal movement.

With the acceleration of urbanization, a large number of coal mines in China engage in mining under villages. The panel formed by underground coal mining is transmitted in the ground via the rock strata, thereby causing damage to the buildings and structures on the surface.

Building movement and deformation are monitored using external methods [terrestrial laser scanning (TLS), total station, and differential level] to master the mechanical state of internal structures and walls in ground deformation areas. On the basis of deformation, a numerical simulation software is used to analyze the internal mechanical state of buildings. Understanding the internal stress state of an intact or slightly damaged building can guide its reinforcement and prolong its life. It can also support the design of anti-deformation buildings through simulated reference data and provide a basis for the design of anti-deformation houses.

In recent years, TLS and other auxiliary methods have been utilized to detect deformation and damage in objects such as bridges, dams, buildings, and landslides (Table 1). The traditional differential leveling, close-range photogrammetric survey, and interferometric synthetic aperture radar

✉ Xugang Lian
lianxugang@tyut.edu.cn

¹ School of Mining Engineering, Taiyuan University of Technology, Taiyuan 030024, Shanxi, China

² School of Geoscience and Surveying Engineering, China University of Mining and Technology, Beijing 100083, China

³ School of Civil and Environmental Engineering, University of New South Wales, Kensington, Sydney, NSW 2025, Australia

Table 1 Some monitoring methods on ground disaster and subsidence

Authors	Monitoring method	Objectives
Maurizio and Margherita (2013)	TLS and GPS	Landslide
Zhou et al. (2014), Zhao et al. (2016) Lian and Hu (2017)	GPS/TLS	Ground disaster induced by underground coal mining
Xu et al. (2014), Kashani et al. (2015) Selbesoglu et al. (2016), Vacca et al. (2016)	UAV, TLS, and Lidar	Damaged or deformed buildings
Valenca et al. (2017), Watson et al. (2013), Burcu et al. (2015), Puente et al. (2014)	TLS	Bridge, breakwaters
Desir et al. (2018)	High-precision differential leveling	Sinkhole subsidence
Al-Halbouni et al. (2017)	Close-range photogrammetric survey	Ground subsidence
Ghazifard et al. (2017), Bignami et al. (2018), van der Horst et al. (2018), Liosis et al. (2018)	InSAR	Ground subsidence

(InSAR) technique are also used to monitor ground subsidence, and some applications are shown in Table 1.

Numerical simulation has been utilized in many areas of mining research (Table 2). Mining methods include long-wall mining, partial mining, and so on. Software for numerical simulation includes commercial types (e.g., FLAC3D, ANSYS, ABAQUS, COSFLOW, and UDEC) and self-developed types (e.g., discrete element and finite-element method). Numerical simulation of long-wall mining is performed to study the evolution of rock strata and surface displacement, whereas that of partial mining is conducted to study the stability of coal pillar and the deformation law of strata and surface.

Underground mining extraction causes deformation of the rock mass and the surface, which may cause damage to the construction of house foundation and other facilities. To consider the interaction between the manhole and the

horizontally strained soil, Zięba and Kalisz (2019) studied the impact of horizontal soil strain on flexible manhole riser deflection based on laboratory test results. Use of a sliding joint is an effective method to decrease the stress in foundation structure where there is a horizontal deformation of subsoil or horizontal deformation of a foundation structure, Cajka et al. (2011) found that temperature is dependent with shear resistance, and the sliding joint shear resistance as a function of deformation velocity and temperature, which is used for the numerical analysis of stress/strain relation between foundation structure and subsoil. Deck et al. (2003) described soil–structure interaction phenomena at work during a mining subsidence. A finite-element software is used to generate models incorporating the ground material and a supported rigid structure. The structures are loaded in particular by ground curvature and strain. The cases where ground movements are integrally imparted to the structure

Table 2 Studies that performed numerical simulation of underground mining

Author	Mining method	Software	Purpose
Iwanec et al. (2016)	Long-wall mining/ long-wall top coal caving mining	ABAQUS	To investigate the subsidence profiles predicted above single and multi-seam long-wall panels
Adhikary et al. (2016)		COSFLOW	To assess the performance of 2D and 3D numerical simulations
Jiang et al. (2018)		FLAC3D	To determine the effect of residual deformation on buildings
Basarir et al. (2015)		FLAC3D	To predict the stresses around the tail and main gates of an underground coal mine
Guo and Xu (2016)	Wongawilli strip	FLAC3D and ANSYS	To study the rules of overlying rock and surface displacement
Lokhande et al. (2018)	pillar mining/bord	FLAC3D	To study pot-hole subsidence due to shallow underground coal mining
Salmi et al. (2017a, b)	and pillar/sublevel caving	DEM	To conduct numerical analysis of a large landslide induced by coal-mining subsidence
Salmi et al. (2017a, b)		FLAC3D	To explore the effect of gradual deterioration on the long-term stability of shallow abandoned room and pillar coal mines
Cao et al. (2016)		UDEC	To identify the stress field and displacement field changes of different sublevel stopping systems for iron mine
Zhang and Lehane (2019)		Finite element	To examine the relative influence of key factors controlling the stability and surface deformations of shallow, horizontal coal mine panels overlain by sedimentary rock

are distinguished from those showing a strong interaction. The problem is simplified by dissociating the ground curvature and the strain. Chang et al. (2011) used the finite-element models ANSYS and given the soil–structure interaction phenomena produced at the interface between the reinforced concrete structure and the soil have been used to perform a parametric study of the strengthening design of the foundation and the sluice chamber within mining subsidence area.

In the underground coal-mining area, the external surface of the disturbed building and the ground monitoring are studied separately, and a lot of numerical simulation is used to study the stress and displacement of the building. There is a lack of a combination of them. Therefore, the influence of the ground movements of the coal-mining area on the internal mechanics and the displacement state of the building is the focus of this paper.

External monitoring of houses in subsidence area

Geological and mining condition

The study area is located in Huainan, north-central Anhui Province, China. Huainan is a coal enrichment area. Huainan has 15.3 billion tons of proved coal reserves and 44.4 billion tons of prospective reserves, accounting for 71% of the total coal reserves of Anhui Province and 32% of that of east China. It is also one of China’s 13 “billion tons of coal and electricity bases.” Figure 1 displays the location map of the study area.

Panel 16,118 is an underground coal mine panel in Huainan located below the Paifang Village. The strike

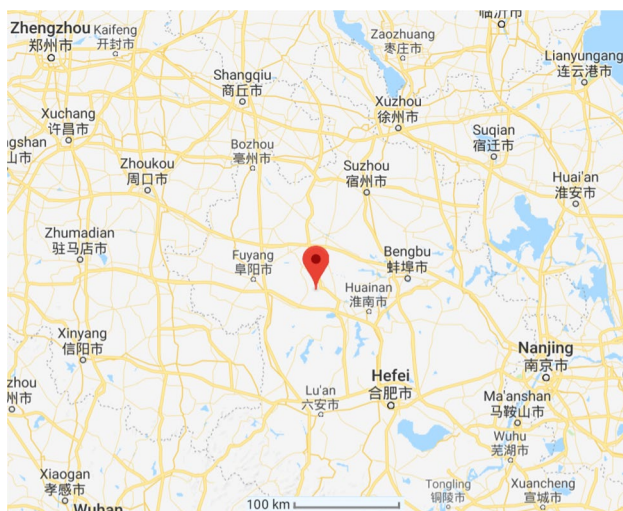


Fig. 1 Location map of the study area

length, incline length, mining depth, and average depth of the loose layer of the panel are 324, 243.7, approximately 450–500, and 300 m, respectively. The extract height and incline angle of the seam are 2.6 m and 10°, respectively. The mining method used is long-wall fully mechanized mining. The period of extraction was 1 September 2009–20 April 2010. Figure 2 shows the geological section.

Figure 3 shows the mining plan and the location of focused measuring houses. House A is located on the outer edge of the panel, and houses B and C are located inside the panel. All three houses are near the stop line and are selected as research objects.

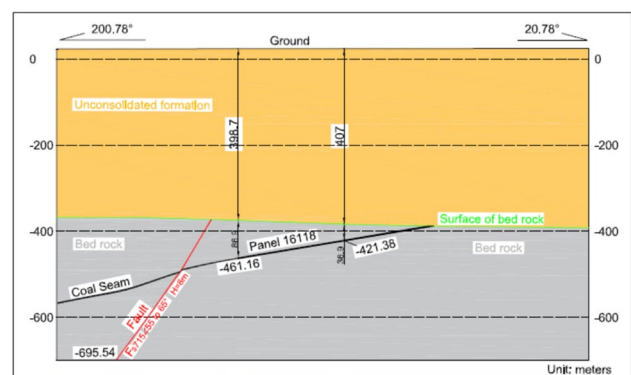


Fig. 2 Geological section

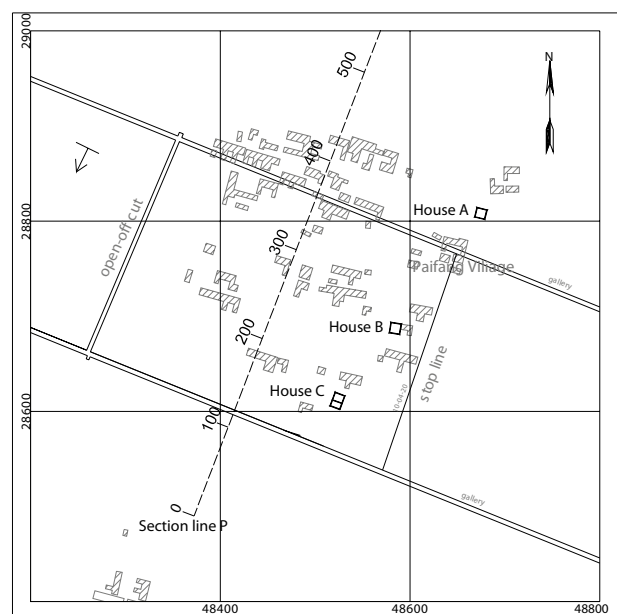


Fig. 3 Mining plan of panel 16,118 and location of measuring houses A, B, and C

Total station and differential level monitoring the houses

Layout of monitoring points and measuring dates

To have a clear understanding of the layout of the measure points around houses A, B, and C, we magnified the layout map, and the layout of the measure points is shown in Fig. 4. Two types of points can be observed: house measure points (in the wall and above ground about 80 cm) and ground measure points (in the ground and distance to the wall about 150 cm).

Houses A, B, and C were monitored seven times on 31 December 2009 (panel advanced distance of 73 m), 23 February 2010 (185 m), 18 March 2010 (280 m), 20 April 2010 (324 m), 19 May 2010 (stop), 16 July 2010, and 9 October 2010. The monitoring points lie in each wall of the houses to unify the direction of deformation. The starting points were A11, A12, B11, B12, C11, and C12 (Fig. 4); clockwise was the forward direction; and the calculated direction of horizontal movement was the azimuth along each wall.

Movement and deformation of the houses

Houses A, B, and C are located in three positions in the ground: outside boundary, middle boundary, and inner boundary of panel. Some differences in movement and deformation exist among the houses. The below analysis is based on the data of 9 October 2010, as shown in Table 3. Subsidence was obtained by leveling, horizontal movement was obtained by total station, tilt and curvature were calculated by subsidence, and horizontal strain was calculated by horizontal movement. The maximum subsidence was demonstrated by house C, followed by house B and house A. The largest horizontal movement was exhibited by house B, followed by house C and house A. The maximum tilt was displayed by house B, followed by house C and house A. The maximum curvature was shown by house A, followed by house B and house C. The maximum horizontal strain was depicted by house A, followed by house B and house C.

Therefore, the house in the center of the panel showed larger subsidence but smaller deformation than the two other houses. Meanwhile, the house in the inner boundary of the panel was first affected by tensile strain and then by compression strain in the mining processing, and the subsidence of the wall and ground points was similar. The curvature, tilt, and horizontal movement of the wall points were smaller

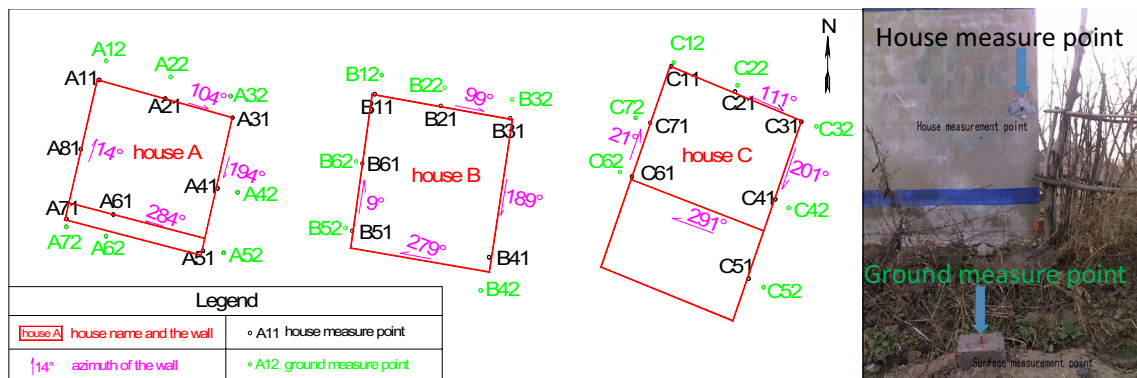


Fig. 4 Layout of house measure points

Table 3 Movement and deformation of house A, B, and C

Movement and deformation	House A		House B		House C	
	Wall	Ground	Wall	Ground	Wall	Ground
Subsidence/mm	622	632	2322	2318	2518	2493
Horizontal movement/mm	636	635	668	709	655	674
Tilt (slope)/mm/m	7.9	-8.1	-9.7	10.9	8.7	-17.6
Curvature/mm/m ²	South-0.4	South-0.2	North--0.2	North--0.3	North-0	North--0.5
	North-0.1	North-0.2	West--0.3	West--0.9	East-0	East--2.6
	East-0.1	East-0.5			West-0	West--1.5
	West-0.2	West-/				
Horizontal strain/mm/m	2.9	6.2	0.7	-9.7	3.1	-9.0

than those of the surface points. The horizontal strain of the houses was smaller than that of the ground, especially the compression strain, where the difference was very large. Based on the observed data, we estimate the subsidence curve of the main section P in dip direction of the panel, which is shown in Fig. 5.

TLS monitoring of the houses

The first scan was conducted on 1 February 2010 when the working face advanced by 87 m and the distance to house C was 165 m. On that date, mining deformation did not affect

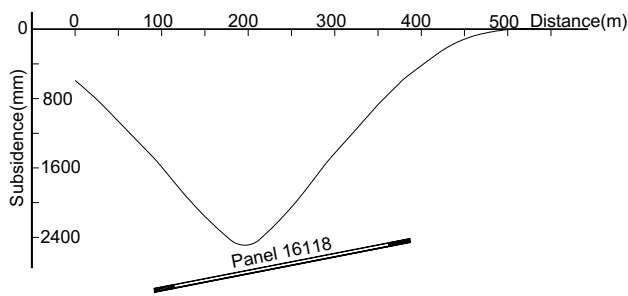


Fig. 5 Subsidence profile of section line P in Fig. 3

all the houses. The second scan was performed on 26 April 2010, which was 6 days after mining stoppage.

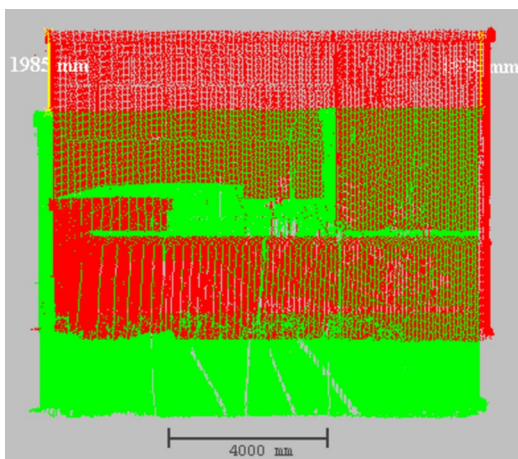
To obtain the absolute coordinates of the two scans, we set up two control points in the stable area outside the affected mining area. Each scan used control points as the starting coordinates, and the coordinates of the monitoring base point were updated by total station traverse surveying.

To obtain the movement and deformation of the building from the point clouds of the two scans, we selected the corners at the top corners of the building as the measuring points. On the basis of the two scans' point clouds, the corner feature point at the top of the building was also used as a measuring point. The data of house C were selected as an example, as shown in Table 4, which lists the vector displacement, movement in the *x*- and *y*-directions, and subsidence of the measured points. The changes in the line were calculated on the basis of the changes in the monitoring distance between the two measuring points.

According to the monitoring data of the three houses, although houses B and C are located in the panel, the movement and deformation of house C were the most severe mainly because of the inclination of the coal seams. Moreover, the center of the subsidence basin shifted to the dip direction of the coal seams.

Table 4 Movement of measuring points in house C

Point number	Vector displacement u_s (mm)	X direction ΔX (mm)	Y direction ΔY (mm)	Subsidence <i>W</i> (mm)	Changes in line (mm/m)
c1	2047	492	124	1984	-2.0
c2	2300	593	101	2220	0.5
c3	2063	513	129	1994	-0.1
c4	1940	485	97	1876	2.9
c5	2002	494	132	1935	2.6
c6	2025	484	111	1963	-2.7



Vertical view of house C



Top view of house C

Point clouds in pre-mining (red) and post-mining (green)

The traditional surveying and TLS for subsidence and horizontal movement are uniform in magnitude and direction. The tilt of the two methods is uniform in direction, but the difference in magnitude is large. In consideration that the feature points lie on top of the house, the tilt is affected by this condition. The difference in horizontal strain is small.

Houses A, B, and C underwent varying degrees of movement and deformation. Their surfaces did not show significant cracks mainly because of the use of structural columns, ring beams, and other strengthening techniques in their construction. The quality of the houses considerably improved during construction. Moreover, no significant cracks were observed on the houses regardless of their stress state. On the basis of the changes in the line of the houses monitored by traditional surveying and TLS, finite-element numerical simulation was performed to evaluate the internal force of the houses in “[Analysis of internal forces on houses caused by line changes](#)”.

Analysis of internal forces on houses caused by line changes

The three houses used in this study have the same basic structure, and the authors used a type of general housing structure in the village to analyze the stress state of the houses. The finite-element software ANSYS was utilized to analyze the model, Table 5 lists the material parameters, and Fig. 6 shows the entire model of the front wall. The left half of the model was modeled and analyzed using the plane element with consideration of symmetry to improve the accuracy and efficiency of the calculation. In the model, the structural column, ring beam, foundation ring beam, strip foundation, and wall were considered, and different material properties were defined. The dimensions of each part of the model are as follows (unit: mm): foundation section, 400×100 ; foundation ring beam section, 400×400 ; structural column, 240×240 ; ring beam, 240×300 ; floor height, 3000; axial spacing of structural column, 3300; window, 1500×1500 ; and wall thickness, 240. In the analysis, the influence of tensile deformation on the front wall under deadweight load was considered. Table 6 lists the analysis conditions.

Table 5 Material parameters of the finite-element model

Item	Material unit	Density (kg/m^3)	Modulus of elasticity (MPa)	Poisson ratio	Uniaxial compression strength (MPa)	Uniaxial tensile strength (MPa)
Foundation section	SOLID45	1800	30	0.25	\	\
Foundation ring beam section	SOLID65	2500	30,000	0.20	22.98	2.10
Wall	SOLID65	2000	2200	0.15	11.50	0.11
Structural column	SOLID65	2500	30,000	0.20	22.98	2.10
Ring beam	SOLID65	2500	30,000	0.20	22.98	2.10

Fig. 6 Finite-element model of front wall

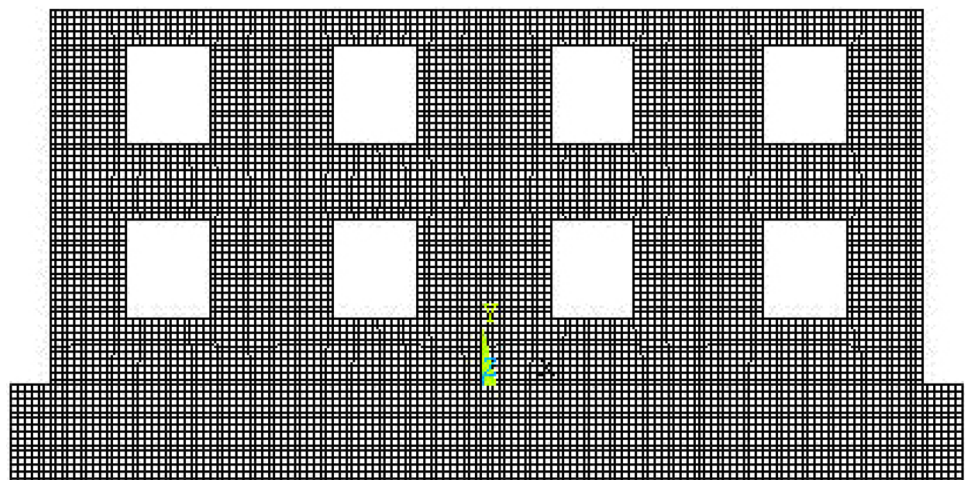


Table 6 Analytical conditions

Type of conditions	Basic condition	Deformation condition
Constraint condition	Vertical UY, horizontal UX	Changes in line X direction
Load	g, q_b	g, q_b
Deformation	–	Changes in line 2 mm/m

Notes: g denotes the weight of the construction member, and q_b indicates the linear load that takes the weight of the plate to the ring beam

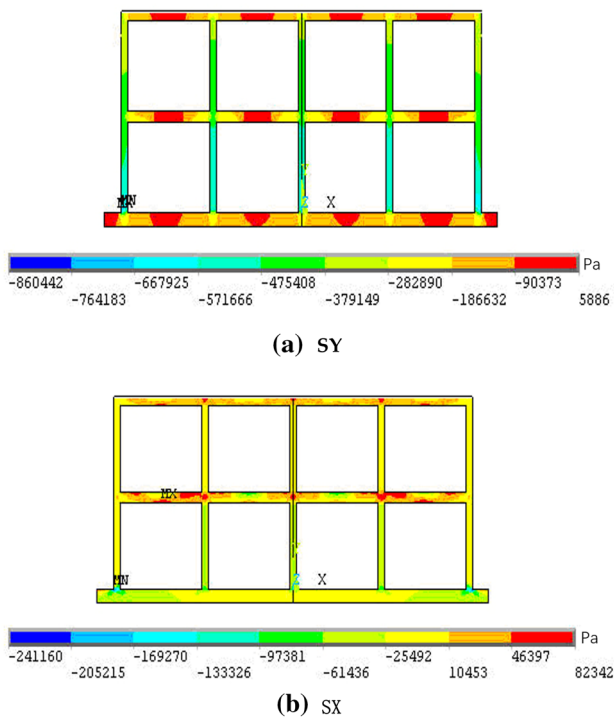


Fig. 7 Axial stresses of structural columns and ring beams under basic conditions (entire wall)

Axial stress of ring beams and structural columns

Figures 7 and 8 shows the axial stresses of the structural columns and ring beams under both conditions, where SX and SY denote the horizontal and vertical principal stresses, respectively. Under the basic condition, the maximum vertical principal stress was concentrated in the middle of the ring beam between the structural columns, and the horizontal principal stress of the second layer was slightly higher than those of the other layers. Under the action of tensile deformation (line changes), the horizontal stress of the foundation ring beam was greatly affected.

Analysis of main stress results of the wall

The maximum principal and maximum shear stresses of the wall were used to evaluate the risk of wall cracking under the two conditions. Figures 9 and 10 present the principal

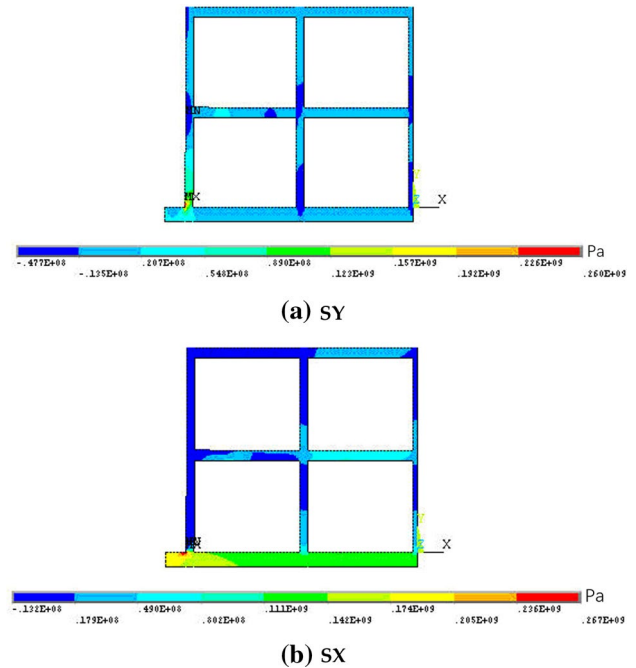


Fig. 8 Axial stresses of structural column and ring beam under deformation conditions (half wall)

stresses of the wall under the two conditions and the maximum shear stresses of the wall under the two conditions, respectively. Table 7 shows that the principal and shear stresses increase proportionally with the increase in tensile deformation. The window corner is the principal point of stress for the wall with a window, where the potential risk of cracking is great.

The foundation ring beam and the inter-story ring beam enhanced the ability of the house to resist the surface movement and deformation, improved the integrity of the house, and reduced the occurrence of cracks, as shown in Fig. 11.

Discussion

The discussion on monitoring results

The houses A, B, and C are respectively located at three positions above the panel, namely, the outer edge, the middle

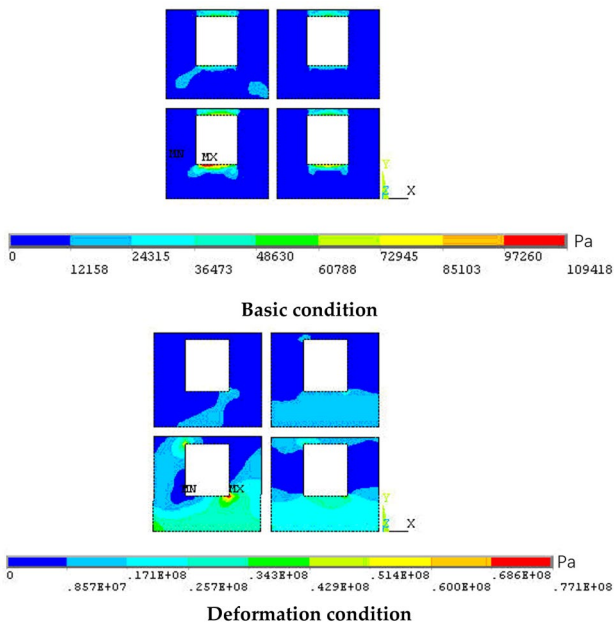


Fig. 9 Principal stress of wall

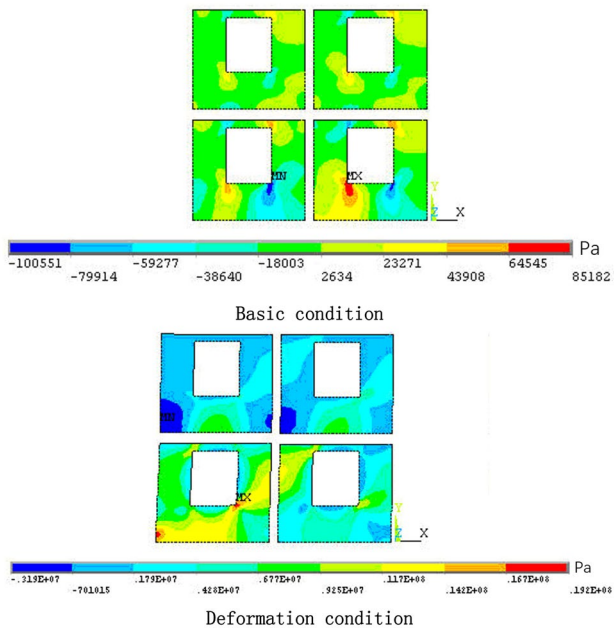


Fig. 10 Shear stress of wall

Table 7 Comparison of results of maximum principal and shear stresses of the wall

Type of condition	Principal stress σ_{max} (MPa)	Shear stress τ_{max} (MPa)
Basic condition	0.11	0.08
Deformation condition	77.1	19.2

part, and the inner edge of the panel. In this study, through monitoring, house C was first affected by underground mining, and its subsidence was the largest. The horizontal movement of house B is the largest, and the tilt of house C is the largest. Building A is located at the edge of panel (ground tensile deformation zone), houses B and C are located at the inside of panel (ground compression deformation zone), and the compression value of house B is larger than that of house C.

Therefore, the general law is that the subsidence of the building in the middle of the panel is larger, but the other deformation values are relatively small. In the mining process, the building is first affected by tensile deformation and then by compression deformation. The subsidence of the building is basically consistent with the subsidence of the ground. Curvature, tilt, and horizontal movement of buildings are smaller than the ground, but the difference is small. The horizontal deformation of buildings is smaller than that of the ground, and the difference is great, especially for the horizontal compression deformation.

The discussion on numerical simulation results

As shown in the numerical simulation section in this paper, when there is no sliding layer of the building foundation, the deformation of the wall is transitive under the action of tensile deformation, which has a great influence on the foundation ring beam and the bottom layer. With the increase of tensile deformation, the principal stress and shear stress of the wall increase proportionately. When there is a window hole, the corner of the window is the key point of stress, and the potential cracking risk is large.

When there is a sliding layer in the building foundation, the sliding layer will reduce the upward transfer of the surface deformation, which greatly reduces the axial stress of the structural column and the foundation ring beam, especially the absorption effect on the tensile deformation. Because the shear slip of the sliding layer consumes the bottom tension of the foundation, the transfer path of deformation is effectively cut off, so that the deformation of the foundation ring beam and the wall is small, the influence of tensile deformation on the stress of the wall is reduced, and the cracking of the wall under tensile condition is effectively slowed down.

The highlights of this study are that the combination of ground monitoring and three-dimensional laser scanning can monitor the building in an all-round way, and the monitoring results can be used to simulate and analyze the internal movement and deformation of the building, so as to determine the internal movement and deformation of the building in the mining area.

The Limitations and future research are: (1) external monitoring by TLS or traditional surveying methods is

Fig. 11 Damaged two-story building with foundation and interlayer ring beam



expensive. Many houses are located in the coal-mining subsidence area, but only three houses are monitored because of monitoring means and financial constraints. The InSAR technique can be used in the future to monitor the deformation of the disturbed houses in real-time and all-weather conditions. (2) The numerical simulation for obtaining the internal mechanical state of the disturbed houses in this study is a general quantitative case, which is based on the monitor results of the three houses. In the future, an automatic system should be developed to combine the deformation results from InSAR and, thus, diagnose the disturbed houses' internal state.

The connection of monitoring and numerical simulation

The construction of the coal-mining subsidence area is easy to observe the external deformation affected by mining, and the stress state of the building and structure is difficult to carry out no damage monitoring. Therefore, the deformation monitoring of the first part of this paper provides the working condition data of building and structure for the numerical modeling of the second part. Particularly horizontal deformation, curvature are sensitive to the building and structure.

The assumption of numerical simulation should be used

In real life, if the quality of the building in the coal-mining subsidence area is good enough, although the building is affected by non-uniform deformation, there is no damage, and the surrounding houses have been cracked or destroyed; at this time, it is necessary to use numerical simulation to evaluate the internal stress state of the exterior intact building to protect it in advance.

Conclusions

1. The traditional surveying (total station and level) and TLS were utilized to monitor the movement and deformation of the disturbed houses affected by underground coal mining. The monitoring results of these two methods are consistent. The external monitoring of the disturbed houses supplies the reference data for the next evaluation of internal force state of the houses by numerical simulation. The influence of horizontal deformation on buildings is more serious, in which the influence of tensile deformation is much greater than that of compression deformation, while synchronous subsidence and movement have no effect on buildings, and tilt has great influence on tall buildings, but relatively little effect on buildings with lower height.
2. Numerical simulation shows that under the action of tensile deformation, the structure of a damaged building in a subsidence zone exerts a considerable influence on the foundation ring beam. An increase in tensile deformation proportionally increases the principal and shear stresses of the wall. The window corners are the principal points of stress when a window exists in the wall, and they are the most at risk for cracking. The brick-concrete structure with foundation sliding layer, reinforced concrete ring beam, and structural column has the best ability to resist surface deformation, and the sliding layer plays an important role in reducing the horizontal deformation of the ground.
3. The combination of external monitoring and internal numerical simulation provides a new way to evaluate the damaged degree of the affected houses by underground mining.

Acknowledgements This study is supported by the National Natural Science Foundation of China (Award Numbers 51704205 and 51574242) and Shanxi Natural Science Foundation of China (Award

Number 201701D221025). We would like to thank Dr. Junting Guo, Dr. Mengguang Liao, and all the surveyors involved in this project for delivering sufficient data.

References

- Adhikary D, Khanal M, Jayasundara C et al (2016) Deficiencies in 2d simulation: a comparative study of 2d versus 3d simulation of multi-seam longwall mining. *Rock Mech Rock Eng* 49(6):2181–2185
- Al-Halbouni D, Holohan EP, Saberi L et al (2017) Sinkholes, subsidence and subsrosion on the eastern shore of the Dead Sea as revealed by a close-range photogrammetric survey. *Geomorphology* 285:305–324
- Basarir H, Oge IF, Aydin O (2015) Prediction of the stresses around main and tail gates during top coal caving by 3D numerical analysis. *Int J Rock Mech Min Sci* 76:88–97
- Bigname C, Brunori CA, Murgia F et al (2018) Multi-sensor monitoring of Ciudad Guzman (Mexico) ground subsidence. *Proc Comput Sci* 138:362–365
- Cajka R, Mateckova P, Janulikova M et al (2011) Sliding joints and soil–structure interaction. *Int J Civ Environ Struct Constr Archit Eng* 5(10):454–457
- Cao S, Song W, Deng D et al (2016) Numerical simulation of land subsidence and verification of its character for an iron mine using sublevel caving. *Int J Min Sci Technol* 26(2):327–332
- Chang H, Xia J, Chang H et al (2011) On the soil–structure interaction numerical study of strengthening design of sluice within mining subsidence areas. *Adv Struct PTS* 1–5(163–167):3640–3644
- Deck O, Al Heib M, Homand F (2003) Taking the soil–structure interaction into account in assessing the loading of a structure in a mining subsidence area. *Eng Struct* 25:435
- Desir G, Gutiérrez F, Merino J et al (2018) Rapid subsidence in damaging sinkholes: measurement by high-precision leveling and the role of salt dissolution. *Geomorphology* 303:393–409
- Ghazifard A, Akbari E, Shirani K et al (2017) Evaluating land subsidence by field survey and D-InSAR technique in Damaneh City. *Iran J Arid Land* 9(5):778–789
- Guldur B, Yujie Y, Hajjar JF (2015) Condition assessment of bridges using terrestrial laser scanners. In: *Proceedings of the 2015 Structures Congress*, Portland, Oregon, April 23–25, pp 355–366
- Guo W, Xu F (2016) Numerical simulation of overburden and surface movements for Wongawilli strip pillar mining. *Int J Min Sci Technol* 26(1):71–76
- Iwanec AMS, Carter JP, Hambleton JP (2016) Geomechanics of subsidence above single and multi-seam coal mining. *J Rock Mech Geotech Eng* 8(3):304–313
- Jiang N, Chen S, Yin D et al (2018) Numerical simulation of building foundation stability above old longwall goaf. In: *9th China-Russia Symposium “Coal in the 21st Century: Mining, Intelligent Equipment and Environment Protection” (COAL 2018)*, Atlantis Press
- Kashani AG, Olsen MJ, Graettinger AJ (2015) Laser scanning intensity analysis for automated building wind damage detection. In: *Proceedings of 2015 Congress on Computing in Civil Engineering*, Austin, Texas, June 21–23, pp 199–205
- Lian X, Hu H (2017) Terrestrial laser scanning monitoring and spatial analysis of ground disaster in Gaoyang coal mine in Shanxi, China: a technical note. *Environ Earth Sci* 76(287):1–11
- Liosis N, Marpu PR, Pavlopoulos K et al (2018) Ground subsidence monitoring with SAR interferometry techniques in the rural area of Al Wagan, UAE. *Remote Sens Env* 216:276–288
- Lokhande RD, Murthy V, Singh KB et al (2018) Numerical modeling of pot-hole subsidence due to shallow underground coal mining in structurally disturbed ground. *J Inst Eng Ser D* 99(1):93–101
- Maurizio B, Margherita F (2013) Monitoring of large landslides by terrestrial laser scanning techniques: field data collection and processing. *Eur J Remote Sens* 46:126–151
- Puente I, Sande J, González-Jorge H et al (2014) Novel image analysis approach to the terrestrial LiDAR monitoring of damage in rubble mound breakwaters. *Ocean Eng* 91:273–280
- Salmi EF, Nazem M, Karakus M (2017a) Numerical analysis of a large landslide induced by coal mining subsidence. *Eng Geol* 217:141–152
- Salmi EF, Nazem M, Karakus M (2017b) The effect of rock mass gradual deterioration on the mechanism of post-mining subsidence over shallow abandoned coal mines. *Int J Rock Mech Min Sci* 91:59–71
- Selbesoglu MO, Bakirman T, Gokbayrak O (2016) Deformation measurement using terrestrial laser scanner for cultural heritage. In: *3rd International GeoAdvances Workshop*, Istanbul, Turkey, October 16–17, pp 89–93
- Vacca G, Mistretta F, Stochino F et al (2016) Terrestrial laser scanner for monitoring the deformations and the damages of buildings. In: *XXIII ISPRS Congress*, Prague, Czech Republic, July 12–19, pp 453–460
- Valenca J, Puente I, Julio E (2017) Assessment of cracks on concrete bridges using image processing supported by laser scanning survey. *Constr Build Mater* 146:668–678
- Van der Horst T, Rutten MM, van de Giesen NC et al (2018) Monitoring land subsidence in Yangon, Myanmar using sentinel-1 persistent scatterer interferometry and assessment of driving mechanisms. *Remote Sens Environ* 217:101–110
- Watson C, Chen S, Bian H (2013) LiDAR scan for blasting impact evaluation on a culvert structure. *J Perform Constr Facil* 27:460–467
- Xu Z, Wu L, Shen Y et al (2014) Extraction of damaged building’s geometric features from multi-source point clouds. In: *International Geoscience and Remote Sensing Symposium (IGARSS)*, Quebec, Canada, July 13–18, pp 4764–4767
- Zhang F, Lehane B (2019) A numerical study to assist assessment of the stability of shallow coal mine goafs. *Geotech Geol Eng* 37(4):2837–2846
- Zhao XP, Zhang J, Liu WL (2016) 3D laser scanning technology in the application of modeling in mining subsidence area. In: *Proceedings of the 6th International Conference on Advanced Design and Manufacturing Engineering (ICADME 2016)*, Zhuhai, China, July 23–24, pp 157–161
- Zhou D, Wu K, Chen R et al (2014) GPS/terrestrial 3D laser scanner combined monitoring technology for coal mining subsidence: a case study of a coal mining area in Hebei, China. *Nat Hazards* 70:1197–1208
- Zięba M, Kalisz P (2019) Impact of horizontal soil strain on flexible manhole riser deflection based on laboratory test results. *Eng Struct*. <https://doi.org/10.1016/j.engstruct.2019.109921>

Publisher’s Note Springer Nature remains neutral with regard to jurisdictional claims in published maps and institutional affiliations.